Lab 1: Signal Acquisition and Processing

Pranav Maddula

Lab Partners: Bryce Maxwell, Andrew Whitaker

Washington University in St. Louis

BME 301A

Lab Instructor: P. Widder

Experiment date: 8/30/2019 & 9/13/2019

Submission Date: 9/24/19

I hereby certify that this report is my own original work: **Pranav Maddula**

Introduction:

This lab exposes the students to the principals of signal processing and key active circuit components. These skills are imperative to hold for any biomedical engineer. In the first part of the Lab, critically important test equipment such as the function generator and oscilloscope are introduced. These tools are used throughout the lab to help analyze and understand other important signal processing elements such as operational amplifiers (op-amps), low-pass filters, and high-pass filters. These included the characterization of differential and common mode gain and input impedance. These concepts were then further hit home through the introduction of signal acquisition theory with the involvement of AC and DC coupling, fast Fourier transforms (FFTs), sampling rate considerations and digital filtering. These concepts are all vital for any technical experiment and are especially important for working with biomedical instrumentation and machinery.

Methods & Materials:

Part one of the lab focuses mainly on the characterization of two op-amps, the INA137, and the INA118. There is also a small section at the beginning focused on getting familiar with the function generator, oscilloscope and oscilloscope probes. This section has the students familiarize themselves with the probe and oscilloscope gain values, noise sources and the voltage stability of the function generator. This is followed by measurements and calculations for the differential gain for both of the op-amps. This is then expanded upon in the next section by measuring and calculating the common-mode gain as well. This is then used to find the common-mode rejection ratio (CMRR) of the op-amps. This section about o-amps is then capped off with a calculation of the input impedance of the op-amp using a decade resistance box to load down the input of the op-amps.

The second part of the lab switches gears to focus more on digital signal acquisition and processing. The first part of this section of the lab focuses on illustrating the differences between AC and DC coupling modes for oscilloscope signal acquisition. This is then followed up with testing of analog, real-world, RC low-pass and CR high-pass filters. These real-world filters were are then tested against the simulated RC and CR circuits from CLab1. The lab then moves to teach digital signal processing via digital filtering in LabChart. This is done by feeding in a constant 5Hz sinusoidal signal and then setting a low-pass filter in software in LabChart. This is then followed by a section about various sampling rates where the same

5Hz signal is acquired using different sampling frequencies in order to better understand the principles of the Nyquist frequency and Nyquist sampling rates. The lab is finally capped off with an exploration of FFTs. These FFTs are used to illustrate the differences between various sample rates and their effect on the digitally reconstructed signal.

Results:

The lab starts by getting the student familiar with the test equipment present, and the limitations of the facilities. In this case, three different pieces of equipment were used; the oscilloscope, the oscilloscope probes, and the function generator. The oscilloscope and probes were tested together using the 'PROBE COMP' port on the oscilloscope. During the tests, the relationship between the probe gain and oscilloscope gain was tested, and the results are as follows:

Probe Gain/Oscilloscope Gain	Resulting Signal (Volts)
1x/1x	2.53 V
1x/10x	25.3 V
10x/1x	256 mV
10x/10x	2.55 V

Table 1: This table shows the relationship between probe gain and oscilloscope gain on the resulting output signal from the 'PROBE COMP' port on the oscilloscope.

We then followed up by testing the function generator in order to get an understanding of the voltage-frequency relationship for our given unit. The results are as follows:

Attenuation/Power Level	-20 dB/Max	-20 dB/Min	0 dB/Max	0 dB/Min
20 Hz	2.10 V	220 mV	22.8 V	2.00 V
200 Hz	2.24 V	220 mV	22.8 V	2.00 V
2 kHz	2.24 V	220 mV	22.8 V	2.00 V
20 kHz	2.22 V	220 mV	22.4 V	1.99 V

Table 2: This table shows the relationship between frequency, attenuation, and power level on the resulting output signal from the function generator. All results were tabulated from the output of the oscilloscope with 1x/1x gain.

Following these measurements, environmental noise was measured using the oscilloscope, and two major sources were isolated. The sources of noise are in the following table:

Noise Source 1	Noise Source 2
20mV, 13.56 kHz: Oscilloscope power supply	10mV, 60 Hz: Touching oscilloscope probe

Table 3: This table shows the amplitude, frequency, and source for two of the most prominent noise sources observed.

For the next part of the lab, the two op-amps were put under initial testing. The first test was calculating the differential gain (G_D) for each of the op-amps. For the INA118, there was a 39 kOhm resistor connected, setting the gain. The gain was calculated using the following formula: $G = \frac{V_{out}}{V_{in}}$ (1). The results are as follows:

	Input Voltage (peak to peak)	Output Voltage (peak to peak)	Gain (G_D)
INA137	1.00 V	2.00 V	2.00
INA118	1.00 V	2.28 V	2.28

Table 4: This table shows the relationship between input and output voltage (peak to peak) and the corresponding gain calculated via equation (1) for both op-amps tested.

Following the differential gain calculation, the transfer function that mapped the relationship between the resistor and the gain for the INA118 was generated. Using collected class data, the curve fitting toolbox in MATLAB was used to generate a regression line relating resistor value to gain. The model is as follows:

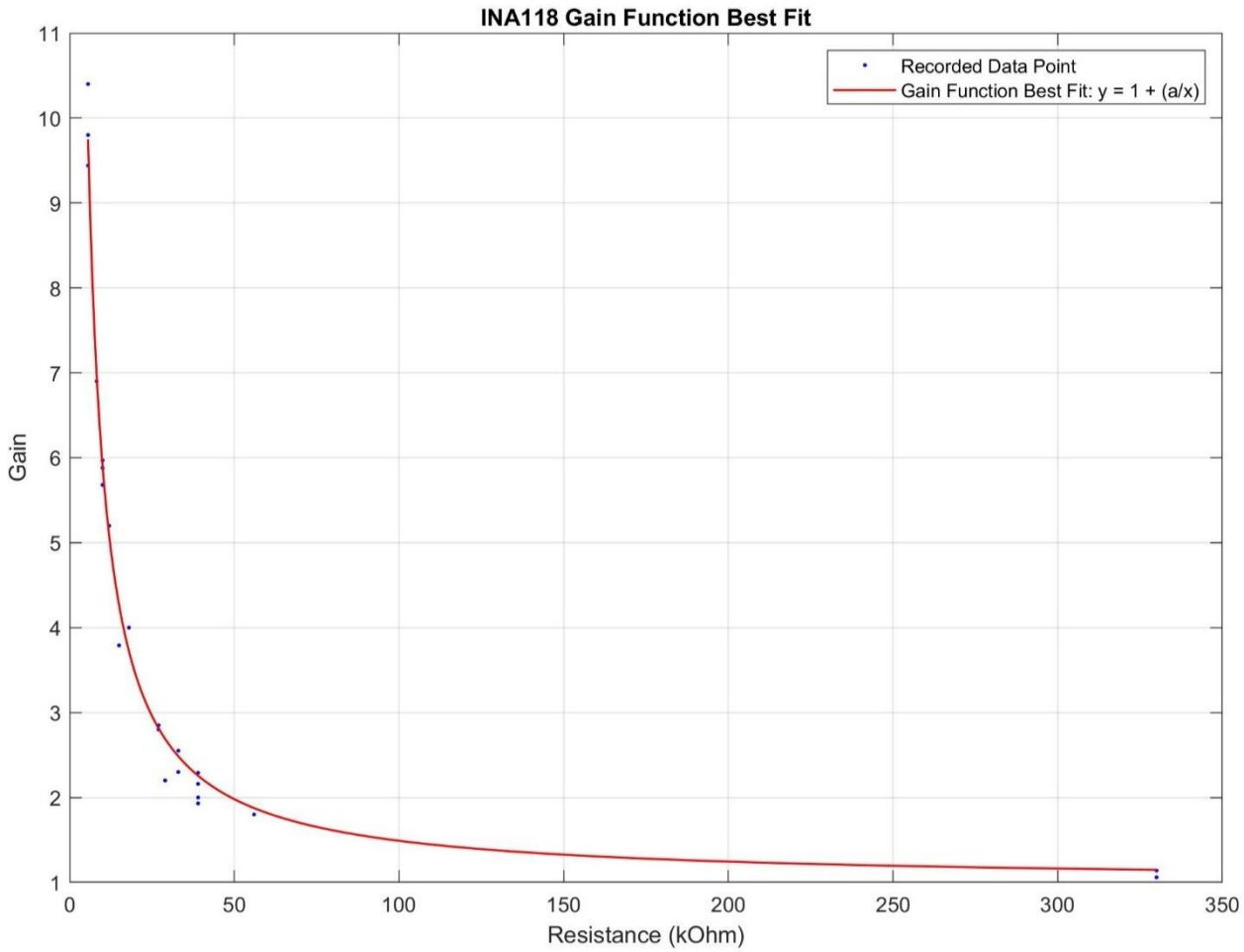

Figure 1: This figure shows the recorded data from the groups (blue) and the regression line (red). The regression equation is y = 1 + (48.99/x), where 48.99 is to 48.99 kOhms. The regression model was set to fit an equation in the form of y = 1 + (a/x). An equation of his form was used in the INA118's datasheet for calculating the gain for any arbitrary resistance.

Next, Common Mode Gain (G_C) for each of the op-amps was tested. Common Mode Gain is also calculated via equation (1); however, the op-amps are re-wired to be in common-mode rejection mode. Using the measured Common Mode Gain, Common Mode Rejection Ratio (CMRR) was also calculated using the equations: CMRR = $\frac{G_D}{G_C}$ (2) & CMRR(dB) = $20Log_{10}(CMRR)$ (3). The compiled results are as follows:

INA137 Common Mode Gain and CMRR

Frequency	Input Voltage	Output Voltage	Common Mode Gain (G_C)	CMRR(dB)	Theoretical CMRR (dB)	% Error
10 Hz	1.00 V	36.8 mV	0.0368	34.7036	~90	61.44%
10 kHz	1.00 V	38.4 mV	0.0384	34.3339	~90	61.85%

10 MHz	1.00 V	48.0 mV	0.0480	32.3957	~60	64.00%

Table 5: This table shows the relationship between frequency, common-mode gain ($\boldsymbol{G_C}$), CMRR and CMRR in dB for the INA137 op-amp. Common-mode gain is calculated via equation (1), while CMRR and CMRR in dB are calculated via equations (2) and (3) respectively.

INA118 Common Mode Gain and CMRR

Frequency	Input Voltage	Output Voltage	Common Mode Gain ($\boldsymbol{G_C}$)	CMRR(dB)	Theoretical CMRR (dB)	% Error
10 Hz	1.00 V	60.0 mV	0.0600	31.5956	~86	60.44%
10 kHz	1.00 V	59.2 mV	0.0592	31.7122	~55	60.32%

Table 6: This table shows the relationship between frequency, common-mode gain ($\boldsymbol{G_C}$), CMRR and CMRR in dB for the INA118 op-amp. Common-mode gain is calculated via equation (1), while CMRR and CMRR in dB are calculated via equations (2) and (3) respectively.

Following this, the lab moved on to characterization of input impedance for the op-amps. Input impedance for an op-amp can be found via the formula: $V_{out} = G \cdot V_{in} = G \frac{R_i}{R_i + R_e} V_{in}$ (4)

Where G is the differential gain G_D**,** R_e is the resistance of the decade resistor box, and R_i is the input impedance. Our results are as follows:

	Input Voltage (Peak to Peak)	Output Voltage (Peak to Peak)	Gain ($\boldsymbol{G_D}$)	Resistance ($\boldsymbol{R_e}$)	Input Impedance ($\boldsymbol{R_i}$)
INA137	1.08 V	800 mV	2.00	90 kOhms	52941.2 Ohms
INA118	1.32 V	1.76 V	2.28	10 MOhms	14.0845 MOhms

Table 7: This table shows the relationship between input and output voltage measured when the decade resistance box is used inline to test for the input impedance R_i of the op-amp. R_i was calculated using equation (4).

Following the characterization of the op-amps, part A of the lab officially finished. For part B, the lab started by exploring the difference between AC and DC coupling in terms of signal acquisition on the oscilloscope. Amplitude was converted from volts to dB via the equation: $\mathrm{dB} = 20 \cdot \mathrm{Log}_{10}(\frac{\mathrm{V_{out}}}{\mathrm{V_{in}}})$ (5)

The observed results are as follows, in a bode plot:

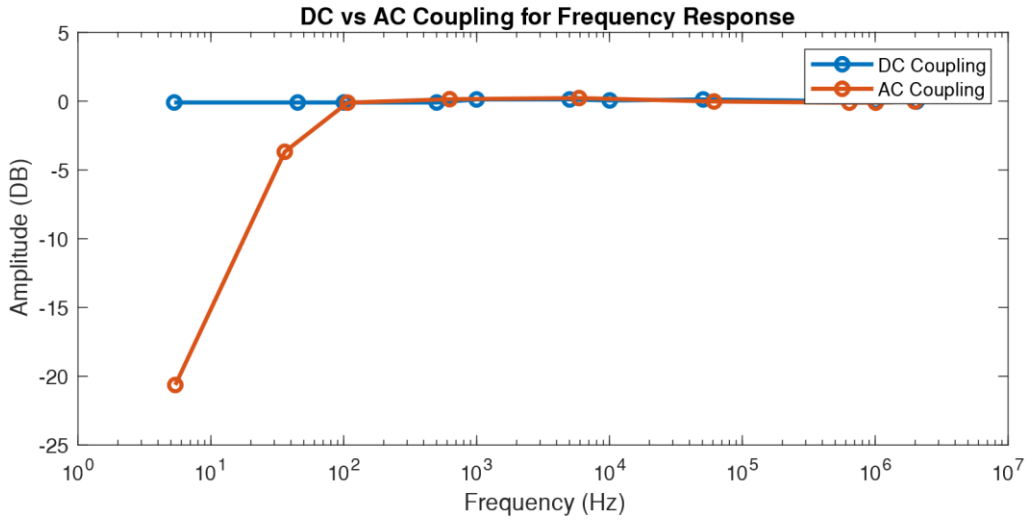

Figure 2: This figure shows the amplitude in dB of the DC and AC coupled signals. Amplitude was calculated using equation (5). AC coupling sees a large decrease in amplitude at low (sub 100Hz) frequencies.

Next, the lab moved on to analyzing the differences between the real world RC & CR filters and compared them to the simulated filters built-in CLab 1. The results are as follows:

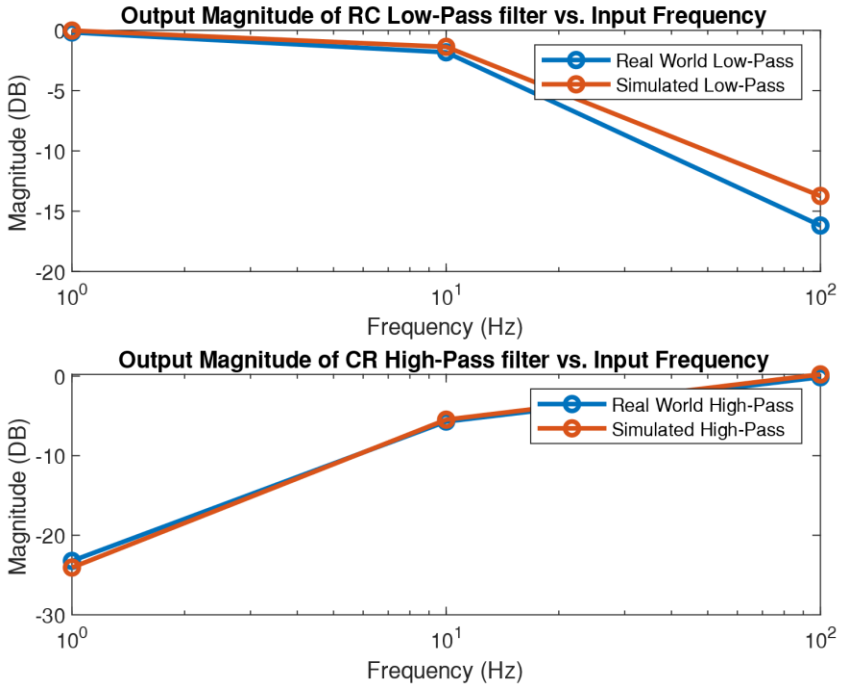

Figure 3: This figure shows the magnitude in dB of the output signal from the real world and simulated filter. The top graph shows data for the RC Low-Pass filter, while the bottom graph shows data for the CR High-Pass Filter.

Both the simulated and real-world circuits utilized the same component values: R = 10 kiloOhm and C = 1 microFarad. Similarly, three frequencies were tested: 1Hz, 10Hz, and 100Hz.

Following this testing of the real world and simulated filters, the lab moves on to testing the discrete-time low-pass filter built into LabChart. The result of the tests are as follows:

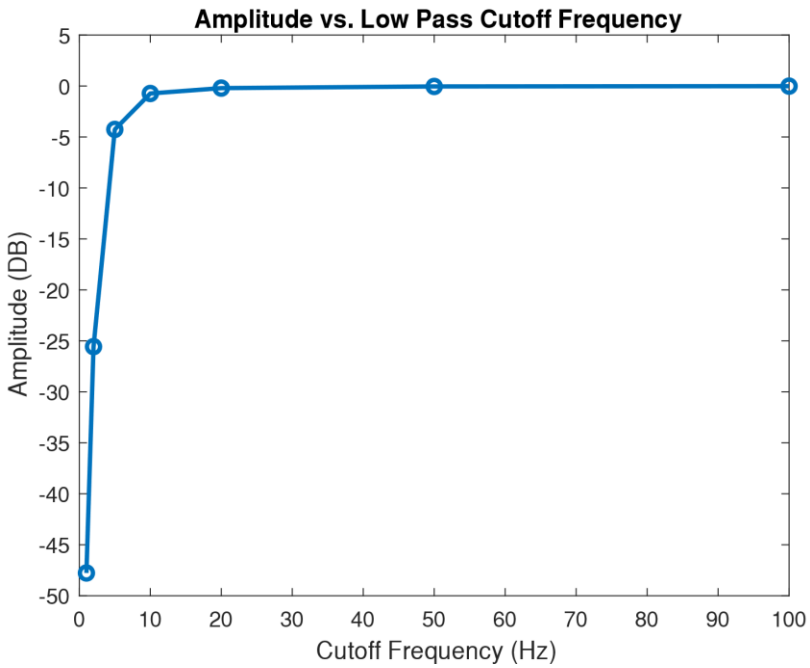

Figure 4: This figure shows the Amplitude in dB of the output signal from different discrete-time low-pass filter cutoffs. The cutoff frequency was selected in LabChart, and seven different values were used: 1Hz, 2Hz, 5Hz, 10Hz, 20Hz, 50Hz, and 100Hz.

A 5Hz sinusoidal frequency, with a roughly 10-volt peak-to-peak amplitude, without a DC offset was used as the input signal for the LabChart filter.

The data for this result is then further analyzed, and the average magnitude, maximum magnitude, and average frequency were extracted, their results are as follows:

Average Magnitude	Maximum Magnitude	Average Cyclic Frequency
-0.2321 Volts	4.7428 Volts	5.4168 Hz

Table 8: This table shows the average magnitude, maximum magnitude, and average frequency exported from the LabChart data. The average voltage is around zero volts as there was no DC offset applied to the signal under test.

Following this section, various sample rates were used to acquire the same signal digitally. The data collected from the various sample rates, along with the average frequency is as follows:

4 S/Sec	40 S/Sec	400 S/Sec	4k S/Sec	40k S/Sec	Average Frequency
1.397 Hz	5.3913 Hz	5.3824 Hz	5.3805 Hz	5.3757 Hz	5.3825 Hz

Table 9: This table shows the acquired frequency at various sample rates. The input signal is constant across the various sampling rates. To note, a 4 S/Sec sampling rate is below the Nyquist sampling rate, and thus the signal is aliased. Thus, this sampling rate is not used to calculate the average frequency.

The final portion of the lab regards Fast Fourier Transforms (FFT) and its ability to extract the various frequency and magnitude components from a given signal. Using the data from the various sampling rates from above, FFT plots were generated and overlaid. The results are as follows

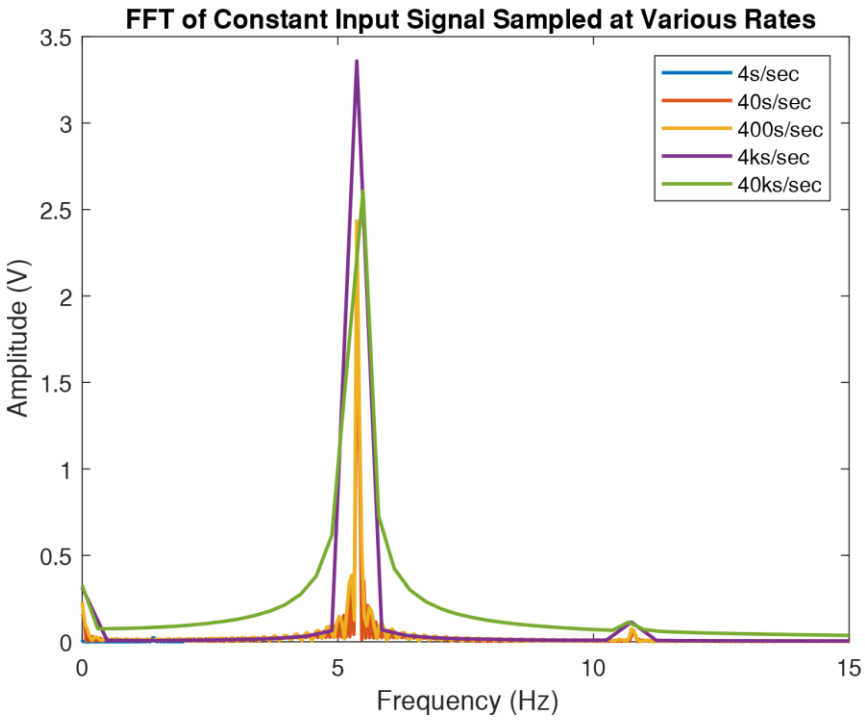

Figure 5: This figure shows the Amplitude in V of the FFTs of the acquired signals at the different sample rates. All of the non-aliased sample rates, show a significant peak around 5Hz, while the aliased sample rate, 4 S/Sec, shows a very small peak around 1.4Hz. All FFTs were calculated with an FFT size of 4K, with the zero-frequency (DC) component remaining.

Discussion:

This lab started with by having the students familiarize themselves with the equipment in the lab. A critical piece of equipment is the function generator, as it generates the signals needed to conduct testing. It can be seen through table 2 that the function generator maintains an essentially stable output across its entire output frequency range. This is desirable behavior as we would like the function generator to operate in a predictable, constant way regardless of how the output frequency changes. This is important as it allows the user not to have to worry about output voltage changes when changing the output frequency.

Through this lab, students also got familiar with the oscilloscope. The oscilloscope to measure noise in and around the workspace, with the results tabulated in table 3. Two relatively large sources of noise were observed, with the first source appearing around the power supply of the oscilloscope. The noise was observed to have a frequency of 13.56 kHz, likely stemming from the switch-mode converter in the power supply. The second source of noise was a 60Hz line noise that was picked up when the probe was touched. This 60Hz noise is likely due to capacitive pickup of AC line power from the human body, and this represents the most pervasive form of noise in the environment we are in.

For the next part of the lab, the gain for the two op-amps were calculated. The INA137 has no external resistor attached to set the gain, while the INA118 has a used an external resistor to set the gain. From the data sheet[1], it can be seen that without a resistor the INA118 gets a gain of 1, however without a resistor, the INA137 has a gain of 2. Thus, the gain resistor bridges a path allowing for a voltage divider to be established inside the op-amp allowing for the op-amp to have variable gain. This theory is confirmed by looking at the op-amp's schematic in the data sheet. The external resistor R_G allows for a voltage path between the input buffer op-amps, establishing a voltage setting the gain.

Following this section of the lab, common-mode gain, and common-mode rejection ratio (CMRR) was calculated. The results from table 5 and 6 shows that the INA137 had a significantly higher CMRR than the INA118. However, looking at the product specifications in the datasheet[1,2] tells a different story. The datasheet for the INA118 claims a CMR of 100dB minimum, while the INA137 datasheet also claims a CMRR of 90dB. However, the data does not back up the datasheet claims. The opposite is seen, with the INA137 having a larger CMRR than the INA118. It is also seen that there is a large across the board reduction in real-world CMRR when compared to the datasheet values for both op-amps, as can also be seen in tables 5 and 6. This is likely due to multiple sources; First and foremost is the fact that the amplifier is quite literally down in the noise. This is the case as the amp is amplifying noise on the input signal that is picked up between the two inputs of the op-amp. This poses a unique challenge as the voltage of the noise we are attempting to pick up and amplify is extremely low for the equipment provided. Another point of concern the resistor in the feedback path of the INA118 op-amp, as the legs of the resistor, can act as an antenna and pick up noise leading to deflated CMRR values.

However, one benefit that the INA118, an instrumentation amplifier has over the INA137, a differential line amplifier is the input impedance. Going back to the datasheet, within the schematic, it can be seen that the INA118 internally is comprised of three op-amps. Two of which are used as non-inverting voltage followers to buffer the input of the final op-amp which is set up as a fixed gain output. This design is contrasted by the relatively simplistic INA137 which is comprised of a single op-amp with a 12 kOhm resistor on each input. These differences are further illustrated with the input impedance specifications listed in the datasheet, where the INA137 has 'only' 24 kOhms of impedance while the INA118 has 10^{10} Ohms, or ten gigaohms of input impedance.

However, once again like above, the observed measurements were off from the figures in the datasheet. For instance, the input impedance value for the INA137 was calculated to be around to 52.94 kOhms, which close to the datasheet value of 24 kOhms. However, our calculated input impedance for the

INA118 is three orders of magnitude smaller than the given datasheet value of 10^{10} Ohms, as can be seen in table 7. This error in both measurements can be mainly attributed to two sources, first of which being the decade resistance box. As the exact resistance of the decade box was not recorded, there may be an error between the markings on the device and the actual reading, leading to skewed results. The second main source of error is specifically for the INA118 reading, as when the INA118 was loaded, an oscillating output was formed. This issue persisted across three different chips including two new devices. This oscillation made it exceedingly difficult to get an accurate voltage measurement.

It can be seen that the input impedance for an op-amp is quite an important property, especially for biological measurement devices. This is the case as the higher the input impedance is, less current flows and thus there is a smaller voltage drop across the source, as voltage drop is proportional to current flow as per ohms law (V = IR). Thus, for biological systems, large input impedance is ideal, as the current flows associated with biological systems are inherently minute; thus even a small amount of current flowing due to a low input impedance will lead to affected measurements. This is also the reason why oscilloscopes have such high input impedances which are usually standardized at 10 MOhms. This large input impedance allows the oscilloscope to probe signals without significantly affecting them.

The next portion of the lab consists of digital signal acquisition. It starts with an exploration of acquisition coupling modes in an oscilloscope. The first figure of this portion, figure 2, shows the different output amplitudes standardized to dB difference across various frequencies for both AC and DC coupling. It can be seen that DC coupling has a steady response across the entire tested frequency, spectrum, while AC coupling appears to have significantly lower amplitudes at low frequencies. From this, it can be inferred that DC coupling implements an all-pass filter, letting all frequencies through equally, while AC coupling implements a high-pass filter. Further, from figure 2, it can also be seen that the cutoff frequency for AC coupling is around 100 Hz. This is exactly what is expected as AC coupling is designed only to let AC signals pass through while blocking DC signals. This is done via placing a capacitor in series with the input to block the DC and let the AC through. However, this also has the effect of attenuating lower frequency AC signals as well. This is contrasted with DC or direct coupling where the entire signal is put through to the acquisition stage of the oscilloscope without any additional filtering or processing.

Following this, the simulated and real-world models of RC and CR circuits were tested, which can be seen in figure 3. From the figure, it can be seen that both the real-world filters tracked the output of the simulated models quite well. However, it is not perfect, as can be seen by the divergence present as the

frequency increases. From this, a few sources of error can be inferred; first, is that the output voltage of the function generator begins to drift as the frequency changes, this may not be a significant amount, but it is enough to change the readings. Second, there is no way the real world resistor and capacitor values are exactly 10 kOhm and 1 microFarad respectively. Thus, the divergence between real-world and simulated components is also another source of error in the readings.

Based on the measured signal used in figure 4, which can be found in table 8, it is expected that at a cutoff frequency of 5Hz, there will start to be a drop off in the output amplitude, which is something that is distinctly seen in figure 4. This is the case as the definition of a cutoff frequency is when attenuation of 3.01dB is seen in the output signal. Thus, it makes sense that at a cutoff frequency, a roughly 3dB reduction of amplitude is seen.

The Minimum sampling rate to be selected should be no less than 2 times larger than the highest frequency component (f_{nyq}) of the signal to be sampled to avoid aliasing. As the data shows in table 9, the frequency of the sinusoidal input is 5.4168 Hz. Thus, the sampling rate should be at least double that, or 11Hz. In the context of the sampling rates tested (as shown in table 9), the best option would be around 400 samples per second. This is the case as the sampling rate is large enough to catch the signal; however, it is not so large as to oversample the data or store too much data. Similarly, it is foolish to use the maximum sampling rate all of the time as doing so produces a large excess of data that makes it hard to store, manipulate and extract useful information from.

The primary peak of the FFT represents the magnitude (height) and frequency (location on the x-axis) of the largest frequency component of the input signal. In this case, the input signal should be a pure sinusoidal wave, and thus should have only one peak. However, a more complex signal will have more peaks. Within the FFTs plotted in figure 5, all of the peaks, except the 4 S/Sec peak exist in a similar region and have similar magnitudes. However, there are still slight differences, with each of the peaks having a slightly differing magnitude and a slightly different frequency, which can also be partially witnessed in table 9. Regardless of the small differences, there is a large outlier, which is the FFT for the 4 S/Sec sampling rate. This FFT has two major issues; first, it has a significantly lower magnitude than all the other FFTs. Second, it has only one peak at around 1.4Hz. This is totally off from the actual input signal, as the input signal is 5.4168, as per table 9. Thus, the 4 S/Sec sampling rate signal is aliased, and the lost signal data is irrecoverable via standard means.

Like stated above, no FFT options could recover the lost data from the 4 S/Sec sample rate as there were not enough samples taken. This sampling rate is even below the frequency of the signal itself, further making it impossible to recover the actual signal from the acquired data points.

Further exploring FFT options, a box for removing the DC component of signals before taking the FFT is provided. This option drops the overall FFT amplitude slightly and also removes the slight peak present at 0Hz (DC). This peak can be seen at the origin in figure 5, and removing the dc component will return that peak to a flat line.

Conclusion:

Overall this lab has the intention of familiarizing the students with the equipment needed to perform basic laboratory tests and further introduces them to the principles of digital signal acquisition and processing. These skills encapsulated in the numerous tests and observations throughout the lab allow the students to build skills that will help them solve complex signals problems and builds a strong framework for understanding the principles underpinning the signal processing tools that will be used for the rest of the students academic careers, and even can be used in the real world.

References:

1. Lab Partners: Bryce Maxwell, Whitaker Andrew
2. Barbour Lectures 1-4
3. *INA118 Precision, Low-Power Instrumentation Amplifier.* Texas Instruments, Apr. 2019. http://www.ti.com/lit/ds/symlink/ina118.pdf
4. *INA137 Audio Differential Line Receiver.* Texas Instruments, Jul. 1997. http://www.ti.com/lit/ds/symlink/ina137.pdf
5. PLab Manual

Unofficial References:

1. Other Individuals were consulted. However, there was no collaboration, only discussion
    a. Students are: Anthony Wu, Spencer Kaminsky, Precious Oluwakemi, Emily Ray
    b. Instructors include: Professor Widder, Professor Ledbetter